Quasicondensation in Two-Dimensional Fermi Gases

Chien-Te Wu, Brandon M. Anderson, Rufus Boyack, and K. Levin

Phys. Rev. Lett. **115**, 240401 — Published 9 December 2015

DOI: 10.1103/PhysRevLett.115.240401

Quasi-condensation in two-dimensional Fermi gases

Chien-Te Wu, Brandon M. Anderson, Rufus Boyack, and K. Levin

James Franck Institute, University of Chicago, Chicago, Illinois 60637, USA

In this paper we follow the analysis and protocols of recent experiments, combined with simple theory, to arrive at a physical understanding of quasi-condensation in two dimensional Fermi gases. We find that quasi-condensation contains aspects of Berezinskiĭ-Kosterlitz-Thouless behavior, including the emergence of a strong zero momentum peak in the pair momentum distribution. Importantly, the disappearance of this quasi-condensate occurs at a reasonably well defined onset temperature. The resulting phase diagram, pair momentum distribution, and algebraic power law decay are compatible with recent experiments throughout the continuum from BEC to BCS.

Understanding two-dimensional (2D) fermionic superfluidity has a long history relating to the Mermin-Wagner theorem [1] and Berezinskiĭ [2], Kosterlitz and Thouless (BKT) physics [3]. More recently it has been viewed as important for addressing the phase fluctuation picture (and related pseudogap phenomena) associated with high-T_c superconductors [4]. Current interest in 2D bosonic superfluids in ultracold atomic gases has revealed a general consistency with the BKT transition [5–7]. For 2D fermionic superconductors and superfluids, however, it should be emphasized that there is some historical controversy [8] (beginning with Kosterlitz and Thouless [3]) surrounding observable signatures and applicability of BKT physics.

Thus recent reports [9, 10] of a form of pair condensation in 2D fermionic gases are particularly exciting. These follow earlier work addressing the ground state [11] and the higher temperature (pseudogap) regime, away from condensation [12]. These latter experiments [12] emphasized that strong normal state pairing (below an onset temperature T^*) is an essential component of 2D Fermi superfluids, even in the BCS regime. Moreover, much of the theory invoked to explain recent condensation experiments [9, 10] was based upon true Bose systems. A characteristic feature of 2D pair condensation at finite T is the presence of narrow peaks in the momentum distribution of the pairs, *without* macroscopic occupation of the zero momentum state. Throughout the paper this will be our definition of "quasi-condensation." Importantly, the associated transition temperature was manifested [9] as a sudden change in slope of a normalized peak momentum distribution for pairs. Moreover, this quasi-condensation in momentum space was associated with algebraic decay [10] of coherence in real space.

In this paper we present a theory of a low temperature 2D Fermi gas and show how it reproduces rather well the results of these recent experiments [9, 10] through an analysis of the phase diagram, the pair momentum distribution and algebraic power law decay. Given the ground breaking nature of the experiments, it is important to have an accompanying theoretical study which follows the same protocols without any adjustments or phenomenology. Our approach is to be distinguished from other studies of 2D Fermi gases [4, 13–24]. In particular, those addressing BKT physics [4, 13, 14, 16, 17, 21], use existing formulae [25, 26] and determine the unknown parameters to obtain $T_c^{\rm BKT}$. In contrast, here we reverse the procedure and follow experimental protocols to thereby provide a new formula, involving composite bosons, for the transition temperature associated with quasi-condensation. In the homogeneous case, this is analytically tractable and presented as Eq. (6) below.

Importantly, there is a rather abrupt crossover out of a quasi-condensed phase at a fairly well defined temperature $T_{\rm qc}$. In the BEC regime this matches earlier theoretical estimates of the BKT transition temperature which are based on different theoretical formalisms [4, 13, 14, 16, 17]. We find that $T_{\rm qc}$ varies continuously with scattering length and, in reasonable agreement with experiment [9], the transition appears at a slightly higher temperature for more BCS-like systems. We infer that the physics driving this quasi-condensation derives from implications of the Mermin-Wagner theorem; that is, from the inability to condense in 2D except at zero temperature. To minimize the free energy, the system remains quasi-condensed for a range of finite temperatures. Since we, as in Ref. [26], make no reference to vortices we *cannot* argue that our observations correspond strictly to a BKT scenario [3], but we can establish that our findings follow rather nicely those of recent experiments.

Background theory.– Theoretical studies of the 2D Fermi gas divide into two classes: those which build on or extend BCS mean-field theory [4, 13, 14, 16, 17, 24, 27], which is the largest class, and those (based on t-matrix schemes) which do not [18–21, 28]. Here we consider a t-matrix theory belonging to the first class. In the following overview we omit technical details which are extensively discussed elsewhere [29, 30], and can also be found in the Supplemental Material [31] along with a comparison to other theories.

To describe the Fermi gas, we begin by introducing a pair propagator $\Gamma(Q)$, representing a Green's function for bosonic, or paired fermionic, degrees of freedom. Here we define the vector $Q = (i\Omega, \mathbf{q})$, where $i\Omega$ is a bosonic

Matsubara frequency at temperature T and $\mathbf{q}$ is the pair momentum. The pair propagator $\Gamma(Q)$ is chosen so that $\Gamma^{-1}(0) = 0$ at a temperature below a true 3D phase transition temperature (where $\mu_{\rm pair} \equiv 0$) and, importantly, we impose the condition that this Thouless criterion reproduces the usual mean-field equation determining $\Delta \neq 0$. In 2D, where $T_c = 0$, this equation at non-zero T is naturally generalized to $\Gamma^{-1}(0) \propto \mu_{\rm pair}$. We emphasize Δ is a pairing gap and not an order parameter.

A key component of the theory is the inclusion of fluctuations, or bosonic degrees of freedom. As we will show, fluctuations in 2D are necessarily unable to condense, thus guaranteeing that $\mu_{\rm pair}$ will never vanish for any $T > 0$. Because $\Gamma(Q)$ represents a pair propagator, it can be expanded at small Q into the generic form:

$$\Gamma(Q) = \frac{a_0^{-1}}{i\Omega - \Omega_{\mathbf{q}} + \mu_{\rm pair} + i\gamma_Q}, \tag{1}$$

and we associate $\Omega_{\mathbf{q}} \approx \hbar^2 q^2/2M_B$ with a pair dispersion of mass M_B. Throughout we find that we can drop the small lifetime contribution γ_Q. Note that the small Q form of the pair propagator is, up to a factor a_0^{-1}, that of a Bose gas which has no direct inter-boson interactions, but in which the bosons interact indirectly via the fermionic medium.

Performing the sum over bosonic Matsubara frequencies $i\Omega$ gives the momentum distribution of bosons defined through $n_B(\mathbf{q}) = -a_0 \sum_{i\Omega} \Gamma(Q) = b(\Omega_{\mathbf{q}} - \mu_{\rm pair})$, where $b(x) = \left(e^{x/k_BT} - 1\right)^{-1}$ is the Bose-Einstein distribution function. From here it is natural to define a boson number density n_B through $n_B \equiv \sum_{\mathbf{q}} n_B(\mathbf{q}) = a_0\Delta^2$, where in the second equality we have associated the number density with the pairing gap. This association is based on the self-energy [29, 30] and addressed in detail in the Supplemental Material [31].

With this formalism we can now determine the unknowns that appear in Eq. (1); we use the generalized gap equation $\Gamma^{-1}(0) = a_0\mu_{\rm pair}$, the bosonic number equation for n_B, and the usual BCS number equation for fermionic density n, given respectively by,

$$\sum_{\mathbf{k}} \left[\frac{1 - 2f(E_{\mathbf{k}})}{2E_{\mathbf{k}}} - \frac{1}{2\epsilon_{\mathbf{k}} + \epsilon_B} \right] = a_0\mu_{\rm pair}, \tag{2}$$

$$\sum_{\mathbf{q}} b\left(\frac{\hbar^2 q^2}{2M_B} - \mu_{\rm pair} \right) = a_0\Delta^2, \tag{3}$$

$$\sum_{\mathbf{k}} \left[1 - \frac{\xi_{\mathbf{k}}}{E_{\mathbf{k}}} \left(1 - 2f(E_{\mathbf{k}})\right) \right] = n, \tag{4}$$

to fully determine our many-body parameters, Δ, μ, and $\mu_{\rm pair}$. Here we define the Fermi-Dirac distribution function $f(x) = \left(e^{x/k_BT} + 1\right)^{-1}$, the single particle dispersion $\xi_{\mathbf{k}} = \hbar^2k^2/2m - \mu$ for a fermion of mass m, momentum $\mathbf{k}$ and chemical potential μ, and the Bogoliubov dispersion with gap Δ which is given by $E_{\mathbf{k}} \equiv \sqrt{\xi_{\mathbf{k}}^2 + \Delta^2}$. We have regularized the gap equation in Eq. (2) by introducing a two particle bound state energy $\epsilon_B = \hbar^2/ma_{\rm 2D}^2$ [24]. To match with experiment, we use a quasi-2D scattering length $a_{\rm 2D}$ parameterized through $\ln(k_F a_{\rm 2D})$. We assume throughout that the transverse confinement is small enough to neglect corrections due to a finite transverse trapping length [32].

At $T = 0$, we can use the well known solution $\mu = \epsilon_F - \epsilon_B/2$, $\Delta = \sqrt{2\epsilon_F\epsilon_B}$ [24] along with $\mu_{\rm pair} = 0$; here $\epsilon_F = \pi\hbar^2 n/m$ is the usual Fermi energy. At finite temperatures, Eq. (3) can be inverted exactly to give:

$$\mu_{\rm pair} = k_BT \ln\left(1 - e^{-n_B\lambda_B^2}\right), \tag{5}$$

where $\lambda_B = \sqrt{2\pi\hbar^2/M_Bk_BT}$ is the thermal wavelength for the composite bosons. The pair chemical potential therefore crucially relies on the bosonic phase-space density $\mathcal{D}_B = n_B\lambda_B^2 \sim 1/T$. At low temperature, $\mathcal{D}_B \gg 1$ and we find an exponential dependence $\mu_{\rm pair}/k_BT \sim -e^{-n_B\lambda_B^2}$. On the other hand, at high temperatures $\mathcal{D}_B \ll 1$ and $\mu_{\rm pair} \sim -T\ln T$ which can be substantial.

Analysis.– The behavior of the pair chemical potential, which we find to be finite and continuous at all non-zero temperatures, underlies the concept of quasi-condensation. That is, there is no true phase transition but rather an abrupt departure from a (quasi-condensed) phase in which $\mu_{\rm pair}$ is exponentially small to one in which it becomes moderately large as T increases. We introduce a tolerance factor ϵ which defines an onset of appreciable $\mu_{\rm pair}$. This is expressed via the fugacity $z = e^{\mu_{\rm pair}/k_BT}$. The departure point from the low temperature exponential occurs when the slope of z with respect to phase-space density is of order ϵ: $dz(\mathcal{D}_B)/d\mathcal{D}_B \sim \epsilon$. This introduces a scale for a smoothed out transition between phases set by a weak (logarithmic) dependence on this tolerance factor $\mathcal{D}_B = \ln(1/\epsilon)$.

Experimentally [9] this quasi-condensation transition is reflected in the momentum distribution of the pairs, $n_B(\mathbf{q})$ via a narrow peak at $\mathbf{q} = 0$ which satisfies $n_B(\mathbf{q} = 0) \equiv n_B(0) = e^{\mathcal{D}_B} - 1$. Thus, we can rewrite the crossover constraint on the fugacity as $dn_B(0)/d\mathcal{D}_B \sim 1/\epsilon$. We find that a threshold in $\mu_{\rm pair}$ enters as a slightly rounded knee in $n_B(0)$. We point out an analogy between this quasi-condensation onset at $T_{\rm qc}$ with the observed [12] pseudogap onset temperature T^* [30]. Both represent abrupt and quantifiable departure temperatures, not associated with sharp phase transitions. Estimates of onset quantities such as T^*, are based on the temperatures at which the deviations become noticeable, say of the order of a few percent.

Using the plots presented in Fig. 1, a graphical analysis of $\mu_{\rm pair}$ suggests that we take ϵ as roughly 1%, reflecting an accuracy in $T_{\rm qc} \approx \pm 15\%$. As discussed in the Supplemental Material [31], a more detailed analysis of fitting functions applied to the correlation function (see Fig. 3, below), also reinforces this estimate of $\epsilon \approx 1\%$.

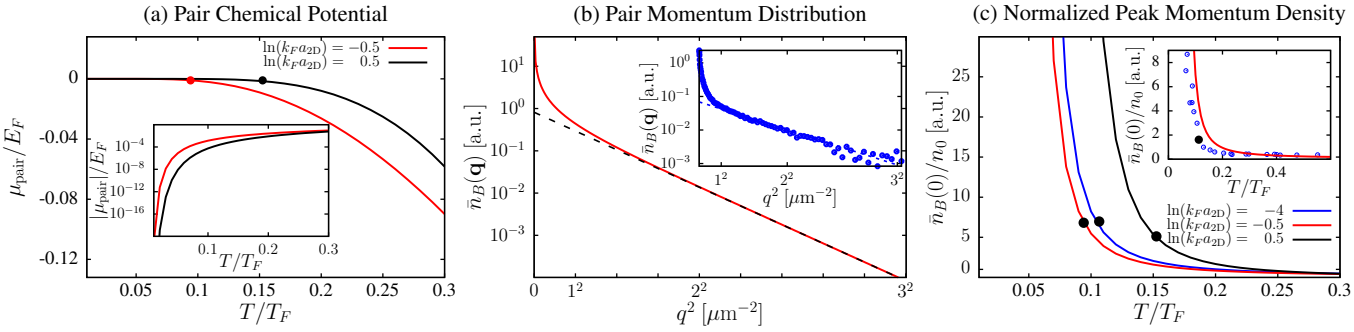

FIG. 1. (a) Quasi-condensation as illustrated via the pair chemical potential, $\mu_{\rm pair}$, as a function of temperature at $\ln(k_F a_{2D}) = \pm 0.5$. Instead of a phase transition there is an abrupt departure from a (quasi-condensed) phase in which $\mu_{\rm pair}$ is exponentially small to one in which it becomes noticeably large. The logarithmic scale inset shows that $\mu_{\rm pair}$ vanishes only at $T = 0$. (b) Normalized momentum distribution at $T/T_F = 0.07$ and $a_{2D} \approx 0.15\mu$m [9, 31]. In the main plot, the red (solid) curve shows the trap-integrated pair momentum distribution. The black (dashed) curve is the trap-integrated interpolation from a corresponding Boltzmann distribution. The inset shows the same quantity from Ref. [9]; the dashed line is a Boltzmann fit to the experimental data at large q. (c) Peaks in the normalized momentum density as functions of temperature for a range of $\ln(k_F a_{2D})$. The black solid circles are $T_{\rm qc}$ determined from Eq. (6). The inset plots experimental data (blue-dots) along with the experimentally determined T_c (black circle) [9]; this is directly compared with theory (red-solid) for closely matched parameters ($a_{2D} \approx 0.15\mu$m). Where relevant, the arbitrary unit scales provide a direct comparison of theory and experiment [31].

This yields

$$k_B T_{\rm qc} \approx \frac{\pi}{2.3} \frac{\hbar^2 n_B(T_{\rm qc})}{M_B(T_{\rm qc})}, \tag{6}$$

and corresponds to $\mathcal{D}_B \approx 4.6$. These values of $\mathcal{D}_B$ are not too different from the Monte Carlo result [33] for a true bosonic gas at the superfluid transition, quoted in Ref. [10] as $\mathcal{D}_B \approx 4.9$ (which corresponds to our $\epsilon \approx 0.7\%$.)

In the deep-BEC regime (where $n_B/M_B = n/4m$) Eq. (6) yields $k_B T_{\rm qc} \approx \frac{1}{9}\epsilon_F$, which is close to estimates in the literature given by $k_B T_c^{\rm BKT} = \frac{1}{8}\epsilon_F$. Importantly, the present expression for $T_{\rm qc}$ applies throughout the BCS-BEC crossover. Towards the BCS limit the number of bosons decreases, but this is compensated largely in the onset temperature by the decrease in bosonic effective mass.

We now extend these analytic arguments to account for trap effects via the local density approximation (LDA). These provide only a minor quantitative change in the general qualitative picture. To apply the LDA, we rewrite our equations in terms of the the local position $\mathbf{R}$, using the transformations $\mu \to \mu(\mathbf{R}) = \mu_0 - \frac{1}{2}m\omega^2\mathbf{R}^2$, $\Delta \to \Delta(\mathbf{R})$, and similarly for all derived quantities; the total atom number is fixed to $N = \int n(\mathbf{R}) d^2\mathbf{R}$. We also define a trap-integrated momentum distribution: $\bar{n}_B(\mathbf{k}) = \int n_B(\mathbf{k}, \mathbf{R}) d^2\mathbf{R}$. When comparing to experimental values, we chose a trapping frequency $\omega = 2\pi \times 18$Hz for a characteristic value of $N = 10^5$ atoms; this corresponds to $T_F \sim 270$nK. For further details of units and the LDA see the Supplemental Material [31].

Comparison with experiment.– We now compare our theory with the recent experimental results in Refs. [9, 10], using our numerical results for the trapped case as "data" analogous to the experiment. In order to probe the momentum distribution of bosonic pairs at low temperatures, in Fig. 1(a) we plot the pair chemical potential versus temperature for two values of $\ln(k_F a_{2D}) = \pm 0.5$, along with an enlarged plot of $|\mu_{\rm pair}(T)|$ which is presented in the inset. The dots illustrate the temperatures associated with the onset; here $\mu_{\rm pair}$ begins to appreciably deviate from zero, thus marking the transition out of the quasi-condensed state.

Figure 1(b) shows an example of the trap-integrated pair momentum distribution $\bar{n}_B(\mathbf{q})$ at $T < T_{\rm qc}$. The small chemical potential $\mu_{\rm pair}$ in Fig. 1(a) results in a sharply peaked distribution $\bar{n}_B(\mathbf{q})$ as $\mathbf{q} \to 0$. The inset presents experimental data [9]. While the agreement with experiment is satisfactory, the differences between experiment and theory suggest that the absolute value of $\mu_{\rm pair}$ we find is somewhat too small.

Finally, we focus on the ratio of the peak magnitude $\bar{n}_B(0)$ of this momentum distribution normalized to the peak number density in the center of the trap, $n_0 \equiv n(\mathbf{R} = 0)$, following the experimental protocol [9]. This is plotted for three different values of $\ln(k_F a_{2D})$ in Fig. 1(c) with the dots indicating the knee (assuming a one percent tolerance factor). This yields our onset temperature in a trap as a function of scattering length. The inset plots the experimental results (indicating their inferred onset temperature) which we overlay on the theory for comparison. For our "data" the transition region is slightly more rounded making it somewhat more difficult to establish a precise onset using only the momentum distribution. Nevertheless the behavior of both around the "knee" is not too dissimilar.

We next use this analysis to obtain the phase diagram as a function of interaction strengths investigated

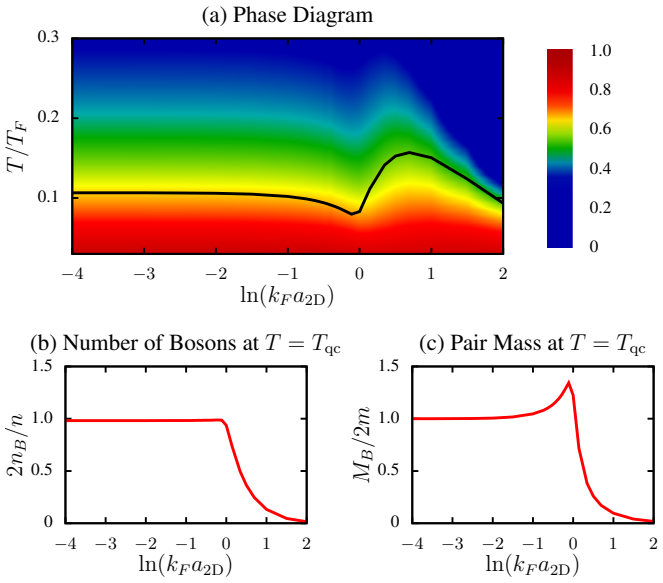

FIG. 2. (a) The phase diagram associated with the quasi-condensation onset (black curve), T_{qc}, as a function of the scattering length $\ln(k_F a_{2D})$. The colored shading represents the non-thermal fraction (see text and Fig. 1(b)). The bosonic number density $n_B(T_{qc})$, and pair mass $M_B(T_{qc})$, at T_{qc} are shown in (b) and (c) respectively. All quantities are calculated from $R = 0$ data in the LDA.

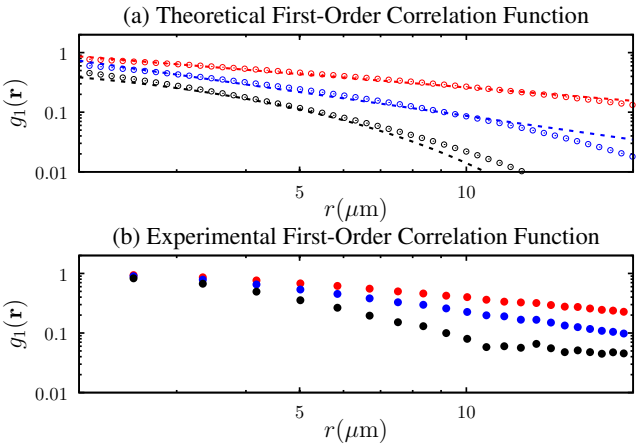

FIG. 3. (a) Theoretical correlation function, $g_1(\mathbf{r})$, in the LDA. We consider three different temperatures at a scattering length $a_{2D} \approx 0.15\mu$m [10, 31], where $T_{qc} = 0.1T_F$. The red, blue, and black curves correspond to, $T/T_{qc} = 0.6$, $T/T_{qc} = 0.9$, and $T/T_{qc} = 1.2$ respectively. For $T < T_{qc}$ ($T > T_{qc}$), the dashed lines correspond to a power law (exponential) fit to the theoretical curve. (b) Experimentally measured [10] correlation function $g_1(\mathbf{r})$. Experimental temperature ratios T/T_c (as defined in Ref. [10]) closely match T/T_{qc} for the theoretical curve of the same color.

in experiment. The results are shown in Fig. 2(a) plotted against $\ln(k_F a_{2D})$. Figures 2(b) and 2(c) indicate the numerator (n_B) and denominator (M_B) components of T_{qc} as shown in Eq. (6) as a function of scattering length. The color coding indicates the non-thermal fraction which is found from Fig. 1(b) as the area between the momentum distribution (solid curve) and its high temperature asymptote (dashed line). As the scattering length is increased, the transition temperature begins to drop before rising to a local maximum and then falling off in the deep BCS regime. While the values are rather similar, this non-monotonic behavior is not as directly seen in experiment, although it is suggested in their plots of the non-thermal fraction. It should also be noted that our theory for the transition temperature is applicable across the entire BEC-BCS spectrum, rather than as two endpoint cases as often studied [13, 21].

Finally, in Fig. 3 we present the correlation function $g_1(\mathbf{r})$ determined from the Fourier transform of the trap integrated momentum distribution $\bar{n}_B(\mathbf{q})$, again following the experimental protocol [10]. We fit to a power law for an intermediate range of r corresponding roughly to that used in the experimental data [10]. We find the power law regime appears slightly more extended in experiment than in theory. With our analytic insight we believe there may be better fits to our "data" based directly on an evaluation of our $\mathbf{q} \to 0$ momentum distribution. These are discussed in the Supplemental Material [31]. Nevertheless, following experiment we find a reasonable fit to a power law at low temperature, $g_1(\mathbf{r}) \sim 1/r^\eta$, and a crossover to an exponential fit at higher temperatures, $g_1(\mathbf{r}) \sim e^{-r/\xi}$. This crossover temperature is very close to T_{qc} as found from Eq. (6). Our power laws, which appear to reflect trap effects, lie in the range of $0.75 < \eta < 1.5$, close to the power laws observed in the experiment of $0.6 < \eta < 1.4$ [31].

Conclusions.– The favorable comparisons between theory and experiment in Figs. 1–3 provide helpful insights into the behavior of 2D Fermi gases. Central to our picture is the relation between the zero momentum peak in the pair distribution function and the small pair chemical potential μ_{pair}. As consistent with the Mermin-Wagner theorem, μ_{pair} is shown to never vanish except at zero temperature. We argue that it is this inability to fully condense in 2D which ultimately drives quasi-condensation. Importantly, with increasing temperature there is a rather abrupt transition from this quasi-condensed phase.

Our approach should be contrasted with contributions to the theoretical literature which address BKT physics [4, 13, 14, 16, 17, 21], by solving for the phase stiffness parameters that appear in the Nelson-Kosterlitz formulae [25] for the BKT transition temperature. We follow the experimental procedure to provide a new formula (see Eq. (6)) for the transition temperature associated with quasi-condensation. We stress that our expression is associated with composite bosons whose mass and number density vary significantly and continuously from BCS to BEC.

Acknowledgments.– This work was supported by NSF-

DMR-MRSEC 1420709. We are particularly grateful to Selim Jochim, Martin Ries, and Puneet Murthy for sharing their data and for helpful conversations regarding their experiment and feedback. We also thank Colin Parker for enlightening discussions.

[1] N. D. Mermin and H. Wagner, Phys. Rev. Lett. **17**, 1133 (1966).
[2] V. Berezinskiĭ, Sov. Phys. JETP **34**, 610 (1972).
[3] J. M. Kosterlitz and D. J. Thouless, J. Phys. C. Solid State **6**, 1181 (1973).
[4] V. M. Loktev, R. M. Quick, and S. G. Sharapov, Physics Reports **349**, 1 (2001).
[5] S. Tung, G. Lamporesi, D. Lobser, L. Xia, and E. A. Cornell, Phys. Rev. Lett. **105**, 230408 (2010).
[6] A. Hadzibabic, P. Kruger, M. Cheneau, B. Battelier, and J. Dalibard, Nature **441**, 1118 (2006).
[7] P. Cladé, C. Ryu, A. Ramanathan, K. Helmerson, and W. D. Phillips, Phys. Rev. Lett. **102**, 170401 (2009).
[8] M. R. Beasley, J. E. Mooij, and T. P. Orlando, Phys. Rev. Lett. **42**, 1165 (1979).
[9] M. G. Ries, A. N. Wenz, G. Zürn, L. Bayha, I. Boettcher, D. Kedar, P. A. Murthy, M. Neidig, T. Lompe, and S. Jochim, Phys. Rev. Lett. **114**, 230401 (2015).
[10] P. A. Murthy, I. Boettcher, L. Bayha, M. Holzmann, D. Kedar, M. Neidig, M. G. Ries, A. N. Wenz, G. Zürn, and S. Jochim, Phys. Rev. Lett. **115**, 010401 (2015).
[11] V. Makhalov, K. Martiyanov, and A. Turlapov, Phys. Rev. Lett. **112**, 045301 (2014).
[12] M. Feld, B. Frohlich, E. Vogt, K. M, and M. Kohl, Nature **480**, 75 (2011).
[13] D. S. Petrov, M. A. Baranov, and G. V. Shlyapnikov, Phys. Rev. A **67**, 031601 (2003).
[14] E. Babaev and H. Kleinert, Phys. Rev. B **59**, 12083 (1999).
[15] N. E. Bickers, D. J. Scalapino, and S. R. White, Phys. Rev. Lett. **62**, 961 (1989).
[16] S. S. Botelho and C. A. R. Sá de Melo, Phys. Rev. Lett. **96**, 040404 (2006).
[17] L. Salasnich, P. A. Marchetti, and F. Toigo, Phys. Rev. A **88**, 053612 (2013).
[18] F. Marsiglio, P. Pieri, A. Perali, F. Palestini, and G. C. Strinati, Phys. Rev. B **91**, 054509 (2015).
[19] M. Matsumoto, D. Inotani, and Y. Ohashi, (2015), arXiv:1507.05149.
[20] R. Watanabe, S. Tsuchiya, and Y. Ohashi, Phys. Rev. A **88**, 013637 (2013).
[21] M. Bauer, M. M. Parish, and T. Enss, Phys. Rev. Lett. **112**, 135302 (2014).
[22] A. M. Fischer and M. M. Parish, Phys. Rev. B **90**, 214503 (2014).
[23] G. Bertaina and S. Giorgini, Phys. Rev. Lett. **106**, 110403 (2011).
[24] M. Randeria, J.-M. Duan, and L.-Y. Shieh, Phys. Rev. B **41**, 327 (1990).
[25] D. R. Nelson and J. M. Kosterlitz, Phys. Rev. Lett. **39**, 1201 (1977).
[26] M. Holzmann, G. Baym, J.-P. Blaizot, and F. Laloë, Proc. Natl. Acad. Sci. **104**, 1476 (2007).
[27] N. Dupuis, Phys. Rev. B **89**, 035113 (2014).
[28] R. Haussmann, W. Rantner, S. Cerrito, and W. Zwerger, Phys. Rev. A **75**, 023610 (2007).
[29] Q. J. Chen, I. Kosztin, B. Jankó, and K. Levin, Phys. Rev. B **59**, 7083 (1999).
[30] Q. J. Chen, J. Stajic, S. N. Tan, and K. Levin, Phys. Rep. **412**, 1 (2005).
[31] See Supplemental Material for more information.
[32] D. S. Petrov and G. V. Shlyapnikov, Phys. Rev. A **64**, 012706 (2001).
[33] N. Prokof'ev and B. Svistunov, Phys. Rev. A **66**, 043608 (2002).
[34] Z. Hadzibabic and J. Dalibard, "BKT physics with two-dimensional atomic gases," in *40 Years of Berezinskii–Kosterlitz–Thouless Theory*, Chap. 9, pp. 297–323.